Chemical Physics 62 (1981) 179–186
North-Holland Publishing Company

FOURTH AND SIXTH SPECTRAL MOMENTS IN FAR INFRARED SPECTROSCOPY

M.W. EVANS
Edward Davies Chemical Laboratories, University College of Wales, Aberystwyth SY23 1NE, UK

Received 30 March 1981; in final form 4 June 1981

The analysis of zero-THz spectra is extended to include fourth and sixth spectral moments. The usual dielectric loss ($\varepsilon''(\omega)$) and power absorption ($\alpha(\omega)/\text{neper cm}^{-1}$) spectral features are supplemented by $\omega^2\alpha(\omega)$ and $\omega^4\alpha(\omega)$. The power of this kind of analysis is illustrated by the fact that there is not one currently available analytical theory that can follow let alone predict the experimental behaviour.

1. Introduction

The spectroscopic study of molecular motion and interaction in liquids has reached the point where the molecular dynamical problem is parameterised using ad hoc assumptions [1–5]. The most difficult aspect of this approach is to minimise the number of free parameters while retaining realism to a maximum possible degree. The free variables cannot usually be defined except on an empirical basis, and may for example involve an equilibrium average or combination of averages taken over high derivatives of velocity or acceleration. Examples include the mean square torque and mean square torque-derivative.

Sufficient range of frequency must be used if the essential differences between the ideas now in the literature are to be extracted. If, for example, dielectric relaxation is to be used the range must extend up to the high frequency wings of the far infrared Poley absorption. Similarly Rayleigh depolarised light scattering measurements [6] should be taken as far as possible into the high *and* low frequency regions of the displacement from the exciting line. These spectral features reveal statistical mechanical details such as memory and intertial effects [1, 4]. In particular the far infrared power absorption coefficient [$\alpha(\omega)/\text{neper cm}^{-1}$] is actually sensitive to those subtleties which serve to distinguish between the various available models, details of which are obscured to a large degree at lower (dielectric) frequencies or alternatively by using measurements only on loss.

The assumptions on which the models of the liquid state are based can be avoided by the use of sum rules [7], which have dealt with the total integrated absorption cross section of either $\varepsilon''(\omega)$, the dielectric loss, or $\alpha(\omega)$. The loss and power absorption coefficient are related by

$$\alpha(\omega) = \omega\varepsilon''(\omega)/n(\omega)c,$$

where $n(\omega)$ is the frequency dependent refractive index and c the velocity of light in vacuo.

In this paper we commence the exploration of the usefulness of sum rules on $\omega^2\alpha(\omega)$ and $\omega^4\alpha(\omega)$, using accurate measurements of $\alpha(\omega)$ in the high frequency wings of the far infrared. The mathematical sum rules can be developed for the asymmetric top in terms of the mean square-torque and the mean square torque-derivative. It is shown that the existing far infrared data are sufficiently accurate in the wings to use the method with $\omega^2\alpha(\omega)$, and in rare cases $\omega^4\alpha(\omega)$.

Having developed these sum rules it becomes possible to use them to eliminate the problem of free parameters when we switch our consideration to the bandshape (or correlation function) rather than the area beneath it.

2. Theory

The starting equation for the analysis is the one for the orientational autocorrelation function $\langle \mathbf{\mu}(t)\cdot\mathbf{\mu}(0)\rangle$ (where $\mathbf{\mu}$ is, for example, the dipole vector) used by Quentrec and Bezot [8]:

$$\frac{\mathrm{d}}{\mathrm{d}t}\langle \mathbf{\mu}(t)\cdot\mathbf{\mu}(0)\rangle = -\int_0^t \langle \mathbf{\mu}(s)\cdot\mathbf{\mu}(0)\rangle K_0(t-s)\,\mathrm{d}s. \tag{1}$$

Later we discuss the physical basis of this equation [9].

It is well known that eq. (1) is a Mori/Kubo type of integro-differential with K_0 a memory function, which is itself an autocorrelation function which can be related to its own memory function with an equation similar to (1). It follows that:

$C_u(t) = \langle \mathbf{\mu}(t)\cdot\mathbf{\mu}(0)\rangle / \langle \mathbf{\mu}(0)\cdot\mathbf{\mu}(0)\rangle$,

can be expressed as the following continued fraction in Laplace space:

$$\tilde{C}_u(p) = \left(p + \cfrac{K_0}{p + \underset{\vdots}{K_1}}\right)^{-1}, \tag{2}$$

with K_0, K_1 etc. as equilibrium averages which are related to molecular dynamical quantities in an increasingly complicated way.

The expansion (2) is by no means universally accepted [10] as being useful or even physically meaningful. Its usefulness depends on how many terms $K_n (n\to\infty)$ can be defined experimentally without recourse to least mean squares fitting; and on how it is truncated. We have evidence that the truncation is more than a mathematical gesture if we are able to relate its consequences to a clearly defined set of mathematical equations representing a model of the molecular dynamics. Tables of such information have been drawn up by Evans et al. [1, 7]. The limits of applicability of eq. (2) have also been explored.

Usually this series is truncated by a constant with the units of frequency but no dependence thereon. This means that the correlation function $K_{n-1}(t)$ decays exponentially. There is no problem in unravelling what this means physically for n up to 2, but we may try to see whether it is practically useful to extend the methodology to higher n in combination with sum rules.

The method used is described in the following steps:

(i) The continued fraction, eq. (2), is approximated successively.

(ii) The spectrum is calculated using $p = -i\omega$ for each approximant.

(iii) In the first approximant there is only one variable γ_0 which is the inverse of the Debye relaxation time, i.e. the peak of the low frequency dielectric loss. All successive approximants are used in such a way as to reproduce exactly this peak frequency. This provides us with the extra information:

$$\mathrm{d}\varepsilon''(\omega)/\mathrm{d}\omega_\mathrm{m} = 0. \tag{3}$$

(iv) Successive approximants contain the variables $K_0, \ldots, K_n$ and γ_{n+1}. For the spherical top it is well known that $K_0(0) = 2kT/I$, where I is the moment of inertia. The approximant:

$$\tilde{C}_u(p) = \left[p + \frac{K_0(0)}{p+\gamma_1}\right]^{-1}, \tag{4}$$

is defined using this [7] and eq.(3) for γ_1.

(v) For the next approximant:

$$\tilde{C}_u(p) = \left[p + \frac{K_0(0)}{p + [K_1(0)/(p+\gamma_2)]}\right]^{-1}, \tag{5}$$

a sum rule for $\omega^2\alpha(\omega)$ may be used for K_1 as an additional source of information. This means that $\tilde{C}_u(p)$ may be estimated without fitting. (vi) The next step is:

$$\tilde{C}_u(p) = \left[p + \frac{K_0(0)}{p + K_1(0)/\{p + [K_2(0)/(p+\gamma_3)]\}}\right]^{-1}, \tag{6}$$

where sum rules for $\omega^2\alpha(\omega)$ and $\omega^4\alpha(\omega)$ theoretically give K_1 and K_2 unambiguously. Unfortunately, the accuracy of high wing data is rarely enough to allow us to estimate with any certainty the area beneath $\omega^4\alpha(\omega)$. Here techcal improvements in instrumental interferometry should help, especially in counteracting problems of baseline determination and band overlap.

(vii) The final approximant to be taken is the one involving $K_0, ..., K_3$, and γ_4. It becomes very difficult to find additional sources of information in this case, and the only feasible method of estimating K_3, even to order of magnitude, seems to be by fitting with K_3 as the variable.

The measure of convergence of using successively more variables is taken in the following senses:

(i) The far infrared spectrum should be describable accurately in all cases, while it remains true that the dielectric loss peak is reproduced exactly.

(ii) There should be an increase across the series $\gamma_0, ... \gamma_n$, i.e. the correlation time of each successive memory function should shorten. Otherwise the physical basis for truncation is undermined, because the nth memory function would not be a fast variable compared with the orientational autocorrelation function itself.

2.1. *Sum rules for the mean square torque and mean square torque-derivative*

These can be constructed from the fundamental relations:

$$C(t) = \int_{-\infty}^{\infty} C(\omega)\, e^{i\omega t}\, d\omega$$

$$= \int_{-\infty}^{\infty} C(\omega)\, d\omega + it \int_{-\infty}^{\infty} \omega\, C(\omega)\, d\omega$$

$$+ ... + i^n \frac{t^n}{n!} \int_{-\infty}^{\infty} \omega^n\, C(\omega)\, d\omega, \qquad (7)$$

where the successive integrals are the required moment of the spectrum. We have

$$C^{(n)}(0) = i^n \int_{-\infty}^{\infty} \omega^n\, C(\omega)\, d\omega, \qquad (8)$$

where $C^{(n)}(t)$ denotes the nth derivative of the correlation function $C(t)$. Eq. (8) is a fundamental theorem relating the even spectral moments of a classical autocorrelation function to its time derivatives at equilibrium ($t = 0$). The even spectral moments of order $2n$ are equal to the time derivatives of order n at the origin of the correlation functions. This implies that a classical correlation function must be expanded as:

$$C(t) = \langle A^2(0) \rangle - \frac{t^2}{2!} \langle \dot{A}^2(0) \rangle + \frac{t^4}{4!} \langle \ddot{A}^2(0) \rangle - ...,$$

where

$$\langle A^2(0) \rangle \propto \int_{-\infty}^{\infty} C(\omega)\, d\omega;$$

$$\langle \dot{A}^2(0) \rangle \propto \int_{-\infty}^{\infty} \omega^2\, C(\omega)\, d\omega;$$

$$...;$$

$$\langle A^{(n)2}(0) \rangle \propto \int_{-\infty}^{\infty} \omega^{2n}\, C(\omega)\, d\omega.$$

Specifically when A denotes the dipole vector $\boldsymbol{u}$ the sum rule for the area beneath $\alpha(\omega)$ has been derived from the asymmetric top by Gordon [11] and in the classical limit by Brot [12]. The result is:

$$\langle \dot{\boldsymbol{u}}(0) \cdot \dot{\boldsymbol{u}}(0) \rangle \propto kT[(u_y^2 + u_z^2)/I_x + (u_z^2 + u_x^2)/I_y + (u_x^2 + u_y^2)/I_z]. \qquad (9)$$

Here u_x etc. are the projections of the unit vector along the dipole moment onto the axis of inertia. The approximate relation to the power absorption coefficient follows as:

$$\left(\frac{V}{N}\right) \int_0^{\infty} \alpha(\omega)\, d\omega = \frac{2\pi^2 \mu_V^2}{3c} \times \left(\frac{u_y^2 + u_z^2}{I_x} + \frac{u_z^2 + u_x^2}{I_y} + \frac{u_x^2 + u_y^2}{I_z} \right), \qquad (10)$$

where N/V is the number of molecules per cm^3 and μ_v the dipole moment.

To develop a sum rule for $\int_0^{\alpha} \omega^2 \alpha(\omega)\, d\omega$ it is necessary to evaluate $\langle \ddot{\boldsymbol{u}}(0) \cdot \ddot{\boldsymbol{u}}(0) \rangle$ for the asymmetric top. This may be achieved following a method originally given by Desplanques [13], starting from the purely kinematic relations

[14–16]

$$\dot{u} = \boldsymbol{\omega}\times \boldsymbol{u}, \qquad \boldsymbol{\omega} = \boldsymbol{u}\times\dot{\boldsymbol{u}}.$$

2.2. *Expressions for loss and permittivity*

We now set up a separate set of equations using microwave and far infrared spectroscopy to supplement the sum rules.

(i) In the first approximation $1/(p+\gamma_0)$ we recover the Debye equations for the loss and permittivity. The maximum of the low frequency dielectric loss lies at $\gamma_0(\equiv\omega_m)$.

(ii) In the next case:

$$\varepsilon''(\omega) = (\varepsilon_0-\varepsilon_\infty)\omega\gamma_1 K_0 \times[(K_0-\omega^2)^2+\gamma_1^2\omega^2]^{-1}, \tag{11}$$

$$\varepsilon'(\omega) = \varepsilon_0-(\varepsilon_0-\varepsilon_\infty)\omega^2[\gamma_1^2-K_0+\omega^2] \times[(K_0-\omega^2)^2+\gamma_1^2\omega^2]^{-1} \tag{12}$$

and using $d\varepsilon''/d\omega = 0$,

$$\gamma_1^2 = [K_0-\omega_m^2][3\omega_m^2+K_0]\omega_m^2. \tag{13}$$

(iii) In the three variable and further cases similar equations are obtainable.

3. Discussion

Several different methods of fitting the data were used involving a non-linear least mean square program of the N.A.G. Library, EO4FAA. In the three variable case we iterate on K_1 only, because K_0 is defined by $\langle\dot{u}^2(0)\rangle$. We use for $CHCl_2$ $\varepsilon_0 = 9.08$ and for ε_∞ take $n_D^2 = 2.03$. Of course γ_2 is related to K_1 through eq.(2). The least mean squares best fit is shown as the solid curve of fig. 1 with $\gamma_2 = 2.2\times10^{13}\ s^{-1}$; $K_1 = 5.35\times10^{26}\ s^{-2}$. This compares with $K_1(0)$ derived from the experimental second moment of $3.56\times10^{26}\ s^{-2}$ (in 10% decalin solution, see appendix).

We note the following:

(i) $\gamma_2 > \tau_D^{-1}$, the inverse of the Debye relaxation time. The decay time of the exponential correlation function $K_1(t)$ is therefore much shorter than that of $\langle\boldsymbol{\mu}(t)\cdot\boldsymbol{\mu}(0)\rangle$, the dipole a.c.f. The basis of the continued fraction approach is valid in this case.

(ii) The constraint imposed by eq. (17) shows up as a shoulder in the theoretical best fit curve at low frequencies. The theoretical maximum lies at a higher frequency than that observed.

In the four variable and subsequent cases we have used the following approaches to test the convergence of the continued fraction.

Firstly, in the four variable case K_0 and K_1 are taken as defined by the three variable fit, and γ_3 is related to K_2 via eq. (21). The $\alpha(\omega)$ data are then best fitted by least mean squares using K_2 as a variable.

Secondly, the same procedure was followed by iterating simultaneously on K_1 and K_2.

The curves from these time fittings are almost identical with each other and with that from the three-variable fit. The value of K_1 changes very little between the three- and four-variable fittings and $\gamma_3 > \gamma_2$. The algebraic criteria for convergence of the continued fraction is obeyed. However, it is not possible to define K_2 with any accuracy using this procedure because large variations in K_2 have very little effect on the theoretical $\alpha(\omega)$ curve. This is true when fitting $\alpha(\omega)$ (fig. 1), $\omega^2\alpha(\omega)$ or $\omega^4\alpha(\omega)$. The shortcomings of both the three and four variable theory are clearly revealed in that $\omega^2\alpha(\omega)$ reaches a plateau level in the three and four variable theories, despite the fact that the return to transparency in this case is theoretically ω^{-2} dependent.

Thirdly the moment spectra $\omega^2\alpha(\omega)$ and $\omega^4\alpha(\omega)$ were fitted using the same methods (fig. 2). Again K_1 is well defined but K_2 is not.

The only incisive method for estimating both K_1 and K_2 with reasonable accuracy therefore seems to be by moment analysis, using an iterative method to extrapolate the experimental $\omega^2\ \alpha(\omega)$ data on the high frequency side. This gives us $K_1 = 3.56\times10^{26}\ s^{-2}$; $K_2 = 6.95\times10^{2}$[illegible] with an uncertainty of about ±10% in the former and ±30% in the latter (see appendix).

In the remaining part of this discussion we concentrate on the extra information available from $\omega^2\alpha(\omega)$ spectra under a range of conditions. The Fourier transform of this curve results in an estimate of the normalised rotational acceleration autocorrelation function

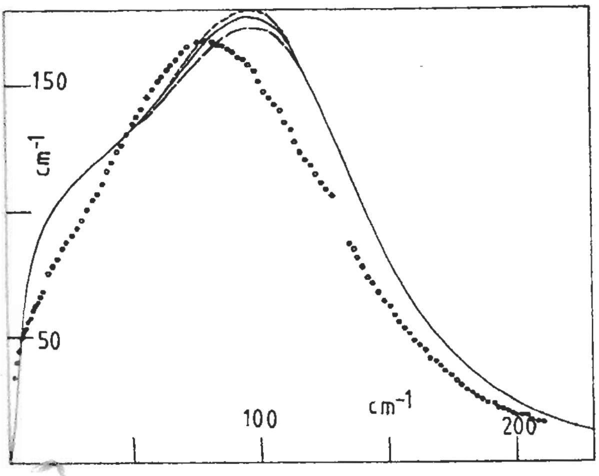

Fig. 1. Mori continued fraction fittings to power absorption data for liquid CH_2Cl_2. ⊙ Experimental data. —— Three-variable fit, taking K_0 as defined by the classical root mean square angular velocity. With ε_0 (experimental) $= 9.08$; $n_D^2 = 2.03$, where n_D is the refractive index of the CH_2Cl_2 liquid absorption at the high frequency end of the far infrared dispersion range. With reference to the main body of the text, $\gamma_2 = 22 \times 10^{12}\ s^{-1}$; $K_1 = 5.35 \times 10^{26}\ s^{-2}$, non-linear least mean squares fitting with the constraint that $\bar{\upsilon}_m(\varepsilon'') = 3.35\ cm^{-1}$, where $\bar{\upsilon}_m(\varepsilon'')$ is the wavenumber at which peaks the dielectric loss. —— Four-variable fit, indistinguishable from the three-variable fit, iterating on γ_3 and K_2. With the constraint $\bar{\upsilon}_m(\varepsilon'') = 3.35\ cm^{-1}$ we have $\gamma_3 = 3.6 \times 10^{17}\ s^{-1}$; $K_2 = 1.30 \times 10^{28}\ s^{-2}$. - - - Five-variable fit, iterating on γ_4 $(= 1.6 \times 10^{17}\ s^{-1})$ and K_3 $(= 2.35 \times 10^{29}\ s^{-2})$ taking $K_2 = 1.3 \times 10^{28}\ s^{-2}$. - - - Four-variable free iteration on γ_3 $(= 6.34 \times 10^{17}\ s^{-1})$; K_2 $(= 1.75 \times 10^{28}\ s^{-2})$; K_1 $(= 5.4 \times 10^{26}\ s^{-2})$. *Ordinate*: $\alpha(\bar{\upsilon})$/neper cm^{-1}; *abscissa*: $\bar{\upsilon}/cm^{-1}$.

(r.a.a.c.f.)

$\langle \ddot{u}(t) \cdot \ddot{u}(0) \rangle / \langle \ddot{u}(0) \cdot \ddot{u}(0) \rangle$.

Figs. 3a and 3b illustrate the information available for the rotator and liquid phases of 2-chloro-2-nitropropane. The r.a.a.c.f. for the rotator phase is slightly the more oscillatory, and both are *more* oscillatory than the corresponding rotational velocity autocorrelation functions related to the Fourier transform of $\alpha(\omega)$ itself [13]. The result is also in harmony with a computer simulation of $\langle \ddot{u}(t) \cdot \ddot{u}(0) \rangle$ carried out by Evans et al. [15] for N_2. This result has implications for the level at which the Mori continued fraction could be truncated, because the

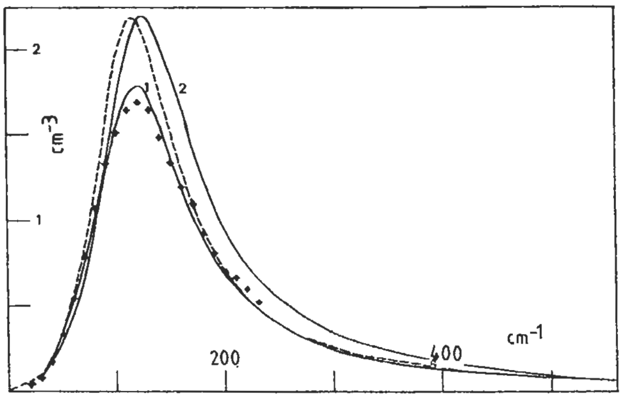

Fig. 2. (1) —— Three-variable fit using ε_∞ $(> n_D^2)$, two variable fit. (2) —— Two-and three-variable fittings using n_D^2. The moment analysis is acutely sensitive to the intensity of the spectrum. - - - Four-variable analysis, using n_D^2. Parameters of fig. 1. *Ordinate*: $10^{-4} \times \bar{\upsilon}^2 \alpha(\bar{\upsilon})$; *Abscissa*: $\bar{\upsilon}/cm^{-1}$.

r.a.a.c.f. is as long-lived as its velocity counterpart. The second memory function, which is defined at $t = 0$ by

$$K_1(0) = \frac{\langle \ddot{u}(0) \cdot \ddot{u}(0) \rangle}{\langle \dot{u}(0) \cdot \dot{u}(0) \rangle} - \frac{\langle \dot{u}(0) \cdot \dot{u}(0) \rangle}{\langle u(0) \cdot u(0) \rangle},$$

is certainly not describable in reality by

$$K_1(t) = K_1(0) \exp(-\gamma t),$$

as in three variable theory, but is inclined to be oscillatory.

Similar behaviour is observable for 2,2-dichloropropane where the $\omega^2 \alpha(\omega)$ spectra show distinctly that the high frequency features in the rotator plane are more pronounced than in the liquid, leading to a more oscillatory r.a.a.c.f.

In figs. 4a and 4b a similar analysis is illustrated for the rotator and liquid planes of *t*-butyl chloride. In this case the opposite behaviour to 2,2-dichloropropane is exhibited in that the liquid $\omega^2 \alpha(\omega)$ spectrum is the broader possibly because in the rotator phase the effects of collision induced absorption are lessened by the symmetrical arrangement of the molecules in the solid lattice. The r.a.a.c.f. is more oscillatory (and longer lived) than that in the liquid.

It is well known that non-dipolar liquids and compressed gases absorb in the far infrared

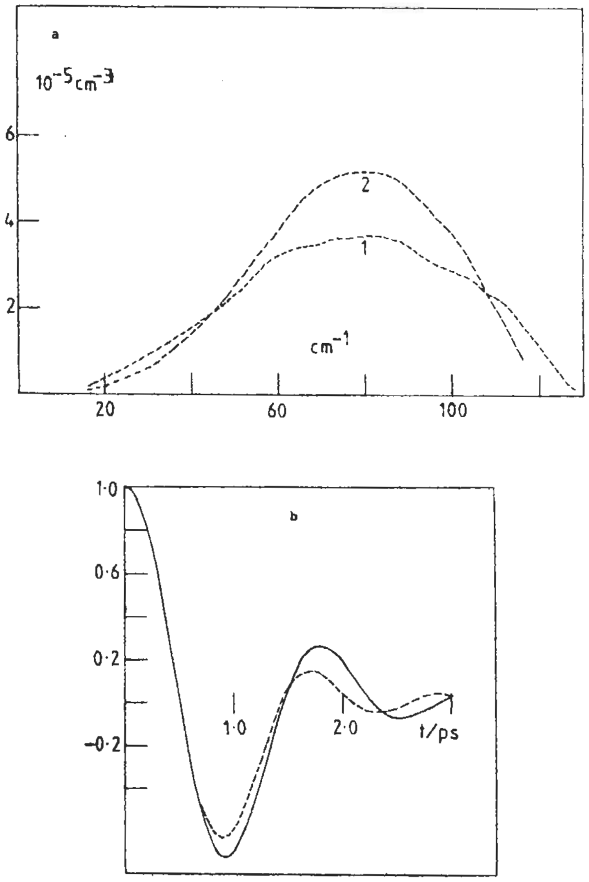

Fig. 3. (a) (1) 2-chloro-2 nitropropane liquid, $\omega^2\alpha(\omega)$ spectrum at 293 K. (2) 2-chloro-2-nitropropane rotator phase $\omega^2\alpha(\omega)$ spectrum at 209 K. *Ordinate*: $\bar{\upsilon}^2\alpha(\bar{\upsilon})$/neper cm^{-3}; *abscissa*: $\bar{\upsilon}$/cm^{-1}. (b) Fourier transform of curves 7(a), —— rotator phase; - - - liquid. *Ordinate*: normalised r.a.a.c.f.: *Abscissa*: *t*/ps.

because of collision induced absorption. The $\omega^2\alpha(\omega)$ of liquid carbon dioxide and its normalised Fourier transform are shown in fig. 5. In principle this type of spectrum could also be used to investigate in further detail the mechanism of dipole induction in a dynamical context. The Fourier transform of $\omega^2\alpha(\omega)$ in this case is also as long lived as that of $\alpha(\omega)$.

In fig. 6 a similar analysis is carried out for liquid CS$_2$, the $\alpha(\omega)$ and $\omega^2\alpha(\omega)$ spectra being compared directly. The effect of uncertainty in the high frequency tail of the spectrum is

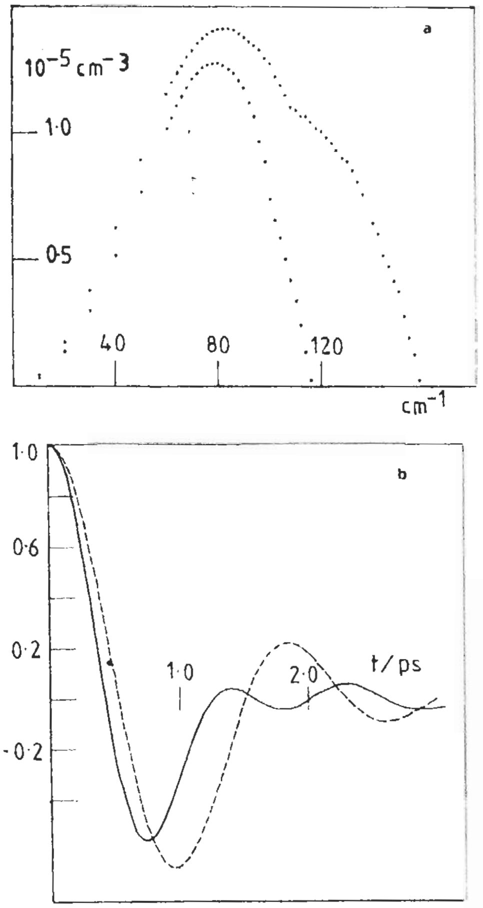

Fig. 4. (a) (1) Rotator phase at 238 K (2) liquid at 274 K (b) - - - rotator phase; —— liquid phase. Ordinates and abscissae as in fig. 3.

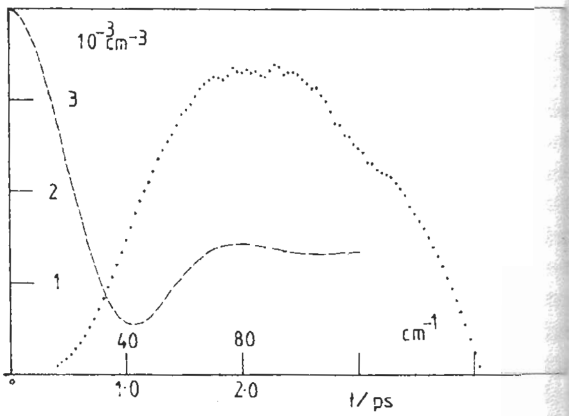

Fig. 5. Liquid carbon dioxide; (a) and (b) ordinates and abscissae as in fig. 3.

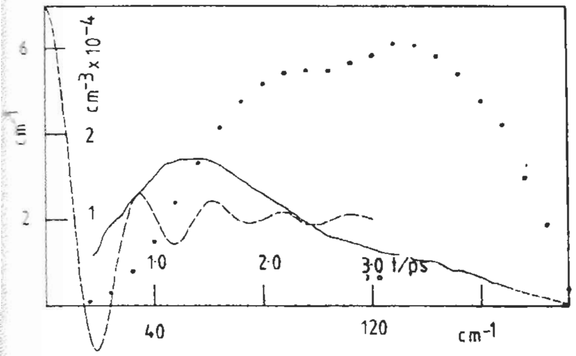

Fig. 6. (a) Liquid carbon disulphide, —— $\alpha(\bar{\upsilon})$/neper cm^{-1} ⊙ $\bar{\upsilon}^2\alpha(\bar{\upsilon})$/neper cm^{-3}. *Abscissa*: $\bar{\upsilon}$/cm^{-1}. (b) Fourier transform of $\bar{\upsilon}^2\alpha(\bar{\upsilon})$, normalised ordinate; abscissa t/ps.

magnified in the $\omega^2\alpha(\omega)$ spectrum, but by no means to an unacceptable degree, so that moment analysis of this kind is generally feasible. The effect of the uncertainty on the Fourier transform is illustrated for benzene in fig. 7.

The new numerical methods currently appearing allow us to evaluate the spectral moments to any order, using, for example, the technique of semi-stochastic simulation, provided the initial equation of motion is properly defined. In this respect a simple Langevin equation for the angular momentum is no longer sufficient.

Acknowledgement

The SRC is thanked for financial support.

Appendix

The Mori continued fraction parameters K_0, K_1 and K_2 can be measured experimentally. In order to present our results in a homogeneous form we have measured with Reid [2, 3] some fresh far infrared spectra for some dipolar solutes in a common environment (decalin solvent). The resulting values of K_0, K_1 and K_2 are thereby assumed to reflect specific solute–solvent interactions, and be unaffected by differing solute–solute interactions as in the main body of the text in this paper. The following values are uncorrected for internal field variation

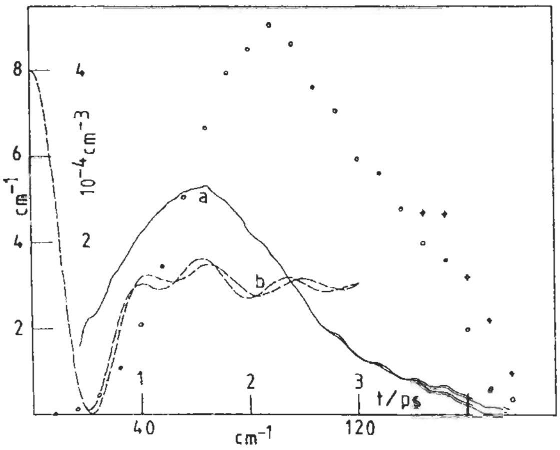

Fig. 7. As for fig. 6, benzene.

Solute (10% v/v except where stated)	10^{-24} K$_0$/s^{-2} (±15%)	10^{-24} K$_1$/s^{-2} (±15%)	10^{-24} K$_2$/s^{-2} (±30%)
CH_2Cl_2	9.29	356	695
$CHCl_3$	17.49	171	479
fluorobenzene	3.70	130	170
nitrobenzene	1.83	143	164
chlorobenzene	5.23	108	152
bromobenzene	7.34	94	172
pentafluoro-benzene	0.94	139	189
1-chloro-naphthalene	1.64	147	233
t-butylchloride	2.52	92	157
pyridine	6.61	211	404
(20%) toluene	7.50	157	190

References

[1] M.W. Evans, G.J. Evans and A.R. Davies, Advan. Chem. Phys. 44 (1980) 255;
M.W. Evans, G.J. Evans, W.T. Coffey, and P. Grigolini, Molecular dynamics (Wiley–Interscience, New York, 1982), to be published.

[2] C.J. Reid and M.W. Evans, J. Chem. Soc. Faraday Trans. II 76 (1980) 286.

[3] C.J. Reid and M.W. Evans, J. Chem. Soc. Faraday Trans. II 75 (1979) 1213.
[4] M. Ferrario and P. Grigolini, Chem. Phys. Letters 66 (1979) 100.
[5] W.T. Coffey, Chem. Phys. Letters 52 (1977) 394.
[6] B.J. Berne and R. Pecora, Light scattering with applications to chemistry, physics and biology (Wiley–Interscience, New York, 1976).
[7] M.W. Evans, Adv. Mol. Rel. Int. Proc. 10 (1977) 201.
[8] B. Quentrec and P. Bezot, Mol. Phys. 27 (1974) 879.
[9] T. Nee and R. Zwanzig, J. Chem. Phys. 52 (1970) 6353.
[10] B.K.P. Scaife, Dielectrics Soc. Conference, Aussois, Piedmont (1980).
[11] R.G. Gordon, Advan. Mag. Res. 3 (1968) 1.
[12] C. Brot, Dielectric and Related Molecular Processes. Chem. Soc. Specialist Per. Rep. 2 (1975) 1.
[13] P. Desplanques, Thèse d'État, University of Lille, France (1972).
[14] M.W. Evans and M. Ferrario, Adv. Mol. Rel. Int. Proc. 19 (1981) 129.
[15] G.J. Wegdam, M.W. Evans and G.J. Evans, Mol. Phys. 33 (1977) 1805.
[16] C.J.F. Böttcher and P. Bordewijk, Theory of electric polarisation, Vol. 2 (Elsevier, Amsterdam, 1978) p. 181.